Brunet and Malvoisin (2025)
Can natural H_2 be considered renewable?
The reference case of a deep aquifer in an intracratonic sedimentary basin
Advances in Geochemistry and Cosmochemistry 1(2): 738, https://doi.org/10.33063/agc.v1i2.738

Research Article

Can natural H_2 be considered renewable? The reference case of a deep aquifer in an intracratonic sedimentary basin

Fabrice Brunet[1] Benjamin Malvoisin[1]

[1] Univ. Grenoble Alpes, USMB, CNRS, IRD, UGE, ISTerre, Grenoble, France

✉ **Correspondence to:** Fabrice Brunet: fabrice.brunet@univ-grenoble-alpes.fr

Author contributions: FB: Conceptualisation, Methodology, Formal analysis, Writing original draft – Review & Editing; BM: Conceptualisation, Methodology, Formal analysis, Writing – Review & Editing.

Submitted: 2025-02-04
Accepted: 2025-06-19
Published: 2025-07-07

Production editor:
James Darling

Handling editor:
Jesse Walters

Reviews:
Frieder Klein,
Anonymous reviewer

Copyediting:
Elliot Carter,
Marthe Klöcking

The possibility that natural H_2, or 'white H_2', can be of economic interest relies on (1) the occurrence of large H_2 gas accumulations similar in size to oil and gas fields and/or on (2) natural H_2 production processes that are sufficiently efficient, locally, to lead to recharge rates that are commensurable with economical extraction rates. This latter possibility is investigated in the reference case of a deep aquifer located in an intracratonic sedimentary basin. Various production reactions are considered which involve RedOx reactions among Fe-bearing rock-forming minerals. The production kinetics of radiolytic H_2 as a function of depth is also modeled. H_2 consumption by microbial activity is implemented. It appears that olivine serpentinisation is the only process capable of generating H_2 concentrations high enough to reach H_2 gas saturation in the aquifer and thus generate H_2-rich gas accumulation. The combination of a deep H_2 source ($>7{,}000$ m, i.e., $T>240$ °C) and a shallow accumulation ($<$ few hundred meters) turns out to be the only possible configuration for such an accumulation. Estimated H_2 accumulation rates do not however exceed a few tons of H_2 per year, which is far from being an economical value estimated to a few kton per year at least. In conclusion, in the case of a deep aquifer in an intracratonic setting and considering water-rock interactions as the main source process, natural H_2 can hardly be considered renewable on an industrial timescale.

1 Introduction

The development of human societies is appending to the resolution of a major antagonism. On the one hand, the growing demand for energy, largely based on fossil fuels, is producing more and more CO_2, and on the other, the accumulation of CO_2 in the atmosphere is the main cause of climate change, the effect of which is an upsurge in climate-related disasters. In this context, H_2 has been seen for long as a 'clean' alternative to fossil fuels. Indeed, (1) H_2 combustion only produces water, (2) H_2 can be produced by electrolysis from renewable electricity (solar, wind, biomass) and (3) H_2 (as well as O_2) can be converted into electricity using a fuel cell, which is considered to be a mature technology.

As part of the energy transition, realistic scenarios suggest using dihydrogen (also called hydrogen hereafter) primarily to decarbonise the industry, in particular where no alternative exists (Oliveira et al., 2021), namely, as feedstock for the chemical synthesis (e.g., Lee et al., 2020), for hydrogen fuel-cell to power heavy-duty vehicles for long driving-range (e.g., Li et al., 2022) or to balance the annual cyclicity in energy demand through seasonal H_2 storage (e.g., Mouli-Castillo et al., 2021). Among these scenarios, green H_2 which is generated from renewable energies (wind and solar) has emerged as one of the best options to fulfill the sustainability requirement unlike H_2 produced from fossil fuels. Yet, if H_2 would be naturally available and exploitable at a level that would meet part of the industrial demand, its status would no longer be an energy vector only, it would become an energy source (Moretti, 2019). Natural hydrogen, formed in the Earth's lithosphere through abiotic geochemical processes, is particularly appealing since its production and accumulation are both natural. In other words, the CO_2 footprint and energy consumption associated with its industrial production would be avoided, making natural H_2, or 'white H_2', a game changer in the transition to a low-carbon economy. Some challenges will obviously arise with the industrial use of H_2 such as the development of large-scale H_2 supply infrastructures as well as public perception and acceptance (e.g., Schönauer and Glanz, 2022). New technical challenges will emerge, in terms of exploration (Moretti et al., 2021a; Lévy et al., 2023) and, H_2 separation and purification (Blay-Roger et al., 2024). Hydrogen exploitation by itself is likely feasible using available oil and natural gas technologies (Blay-Roger et al., 2024).

The notion of natural 'hydrogen system' is regularly described in the scientific literature by analogy with the petroleum system, with its sources, migration routes, reservoirs, seals and traps (e.g., Prinzhofer et al., 2018). The genesis of natural H_2 has been reported in a variety of settings for decades now. Hydrogen emissions in the vicinity of active faults were first described in the early 80s (e.g., Wakita et al., 1980; Sato et al., 1984) and interpreted as resulting from silicates crushing in the presence of H_2O (Kita et al., 1982). At the same time, H_2 emanations were reported in alkaline hydrothermal sources in the Oman and Zambales ophiolites (Neal and Stanger, 1983; Abrajano et al., 1988) which were related to serpentinisation reactions (Moody, 1976). It has long been known that the radiolytic dissociation of H_2O by the decay of radionuclides contained in rocks produces H_2 (Dubessy et al., 1988; Savary and Pagel, 1997) which, in turn, represents a source of energy for the biosphere of the deep Earth's crust (Pedersen, 1997; Lin et al., 2005a).

Despite a vivid (Gaucher, 2020) and long standing (Zgonnik, 2020, references therein) research on natural H_2, and the identification of several natural H_2-forming processes, there is, to date, no recognised natural H_2 exploitable accumulation with sizes which would compare to that of natural gas (hydrocarbon) fields. The H_2 gas occurrence at Bourakeboukou in Mali has become highly emblematic as the only evidence for H_2 accumulation of industrial value, confirmed by a series of wells drilled in the 105 to 1,807 m range (Prinzhofer et al., 2018). There is unfortunately no real evaluation of the H_2 capacity of the Bourakebougou gas accumulation. So far, H_2 was recovered from a single well at a flowing rate of 1,500 standard cubic meter per day (sm^3/day) with an average extraction of 5–50 tons of H_2 per year (Patonia et al., 2024) without significant pressure decrease (Maiga et al., 2023). Thus, regarding the local demand, H_2 can be considered as renewable with a recharge rate of a few tons per year. In terms of order of magnitude, current H_2 production at Bourakebougou remains very low compared with the flow rate of a commercial natural gas well, which is generally in excess of 100,000 sm^3/day (e.g., Ahmed, 2018), bearing in mind that one m^3 of methane under normal conditions contains more than three times the energy of one m^3 of gaseous H_2.

Relatively high H_2 concentrations have been reported in hydrothermal vents at mid-oceanic ridges, in volcanic gases and hydrocarbon fields (e.g., Charlou et al., 2002; Moussallam et al., 2012; Leila et al., 2022, respectively). Besides, disseminated H_2 venting spots have been described in many ophiolite massifs with significant fluxes from ten to hundred kg per year, locally, in bubbling springs from the Oman ophiolite (Leong et al., 2023) and up to above 800 tons H_2 per year in the Zambales ophiolite, Indonesia (Aquino et al., 2025). Among the highest reported outgassing rates, a minimum of 200 tons of H_2 per year has been reported in the galleries of an underground chromite mine in Albania (Truche et al., 2024). Diffuse H_2 surface flux in the Oman ophiolite has been estimated to a few tons H_2 per km^2 and per year (Zgonnik et al., 2019) which should be seen as an upper bound (Leong et al., 2023). Several positive H_2 concentration anomalies in soil porosity have also been reported worldwide corresponding to highly diluted H_2, typically at the 50–1,000 ppmv level (Prinzhofer et al., 2019; Lefeuvre et al., 2021; Frery et al., 2021; Moretti et al., 2021b, 2022). For both ophiolitic and continental settings, however, there is still no clear evidence of direct connection to a deeper reservoir of economic interest.

In addition to H_2 accumulations comparable in size to profitable oil and gas fields, small accumulations with a high inflow rate and a relatively high leakage rate to maintain its small volume could also reveal of economic interest. This concept prompted us to develop a conceptual model of H_2 system with source, transport and accumulation, with the aim of estimating natural H_2 accumulation rates using thermochemical (production) and microbiological (consumption) kinetic constraints. The main natural H_2 production processes namely, the oxidation of ferrous iron contained in minerals and the radiolytic dissociation of water were evaluated using relevant thermodynamic and kinetic data. The contribution of microbiological systems either in soils or from deep biosphere was also considered for its strong H_2 consumption potential (Conrad, 1996; Lin et al., 2005a; Harris et al., 2007; Ivanova et al., 2007; Bagnoud et al., 2016; Löffler et al., 2022; Keller et al., 2024). The inferred maximum H_2 accumulation rates were compared to H_2 extraction rates that were calculated to be profitable in the frame of an industrial project. If geological conditions can be defined where natural H_2 accumulation rates compare with economic extraction rates, then H_2 can be considered as renewable under these specific conditions. The notion of 'renewable' here refers therefore to a resource that is naturally produced at a rate comparable to that at which it is extracted for an economic production. Sunlight and wind are typical examples of this type of energy. Fossil fuels, although natural, are non-renewable resources because they are only renewed on a geological timescale. The aim of this study is thus to define possible conditions in the frame of an aquifer in a sedimentary basin, for which natural H_2 could fall into the category of renewable energies.

2 Magnitude of natural and anthropogenic H_2 fluxes

Hydrogen has a lifetime of 2 years in the atmosphere where its average concentration is around 530–550 ppb. The dihydrogen atmospheric cycle involves an annual global flux of around 75 Mt (Novelli et al., 1999; Price et al., 2007; Ehhalt and Rohrer, 2009). The main H_2 sources include photochemical reactions of hydrocarbons (CH_4 and non-methane) in the troposhere as well as fossil fuel and biomass burning (Figure 1). The major sinks are microbial uptake in soils and atmospheric oxidation by OH radicals (Schmidt, 1974; Conrad and Seiler, 1981; Warneck, 1988; Novelli et al., 1999). The magnitude of the anthropogenic contribution to this cycle has been addressed in several studies going back to the early 70s. Firstly, because the anthropogenic flux is

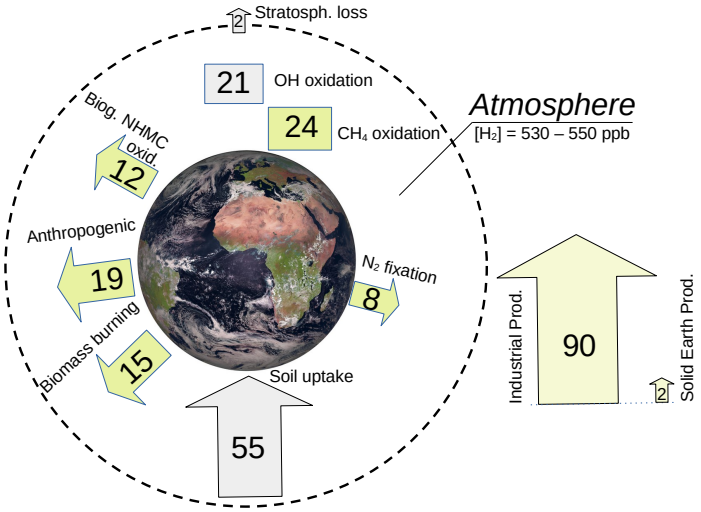

Figure 1. Biogeochemical cycle of atmospheric H_2 highlighting sources and sinks. Sources are in greenish and sinks in greyish color. Data are from Patterson et al. (2020), unit is Mt H_2 per year. Yearly H_2 production for H_2 economy (Industrial Prod., assumed to be independent from atmospheric cycle) and abiotic H_2 production in the Earth's lithosphere (Solid Earth Prod.) are displayed for comparison (Klein et al., 2020). *Biog. NHMC oxid* stands for biological non-methane hydrocarbon oxidation. The Solid Earth production is not integrated to the H_2 atmospheric cycle since a major part of it could be consumed at depth and never reach the atmosphere. Earth image is from EUMETSAT/ESA.

far from negligible (Patterson et al., 2020) and it is likely to increase in the context of a global hydrogen economy. Second, because atmospheric H_2 interacts with the atmospheric cycle of two greenhouse gases, CH_4 and O_3, and could indirectly have an impact on the climate (e.g., Penner et al., 1977; Schultz et al., 2003; Derwent et al., 2006; Ocko and Hamburg, 2022). The anthropogenic contribution related to transportation (fossil fuel combustion) and heavy industry processes was estimated to 15 ± 10 Mt $H_2.yr^{-1}$ (Novelli et al., 1999) which thus represents a major source in the global H_2 cycle. Human activities also contribute to the biomass (and biofuel) burning which is another main source of atmospheric H_2 (Vollmer et al., 2012; Haumann et al., 2013). Besides, the H_2 economy has its own H_2-cycle of production and use, with a global output estimated to 90 Mt.yr^{-1} in 2020 (Aresta and Dibenedetto, 2024). It can be already noted that the H_2-economy cycle is similar in magnitude to the atmospheric H_2 cycle. Besides possible emissions associated with the H_2 production and processing (van Ruijven et al., 2011), these two cycles are expected to be relatively independent.

Natural H_2 coming from the solid Earth has not been considered in the atmospheric H_2 cycle. One reason is that the relevant budget is ill-defined but also because, when estimated, the natural H_2 budget appears to be very small in comparison to other sources. The budget of oceanic H_2 produced by serpentinisation reactions at slow spreading centers is probably one of the best constrained. For a single hydrothermal site like Rainbow on the Mid-Atlantic Ridge, the H_2 discharge is around 200–600 tons of H_2 per year (Charlou et al., 2010). Based on H_2 correlation with ^{3}He and heat on the Rainbow site, Charlou et al. (2010) proposed a total H_2 emission of 0.16 Mt.yr^{-1} for slow-spreading ridges. Independent estimates based on the volume of serpentinised mantle or on total hydrothermal circulation along with vented fluid composition yielded rates in the 0.22–2 Mt.yr^{-1} range (Keir, 2010; Cannat et al., 2010; Worman et al., 2016). While serpentinisation at slow-spreading ridges is recognised as one of the most efficient ways of producing abiogenic H_2 on Earth, its contribution to the global H_2 atmospheric cycle remains relatively marginal.

Similarly, natural H_2 production on the continents is relatively small and is estimated to 0.07–0.45 Mt $H_2.yr^{-1}$ at most (Lollar et al., 2014). In addition, in order to reach the atmosphere, hydrogen produced in the solid Earth needs to go through the efficient microbiological filter in soils, the upper part of which is recognised as a major sink for atmospheric H_2 (e.g., Novelli et al., 1999). Based on our limited knowledge of the magnitude of H_2 produced by water-rock interactions, Klein et al. (2020) proposed a combined production of 2 Mt.yr^{-1} by the solid Earth. Other estimates by one order of magnitude higher (Zgonnik, 2020; Ellis and Gelman, 2024) are based on the tremendous production of H_2 associated with MORB

crystallisation (Holloway and O'Day, 2000), which has yet to be confirmed (Klein et al., 2020).

Yet, even if the annual mass transfer of H_2 from the solid Earth to the atmosphere is clearly marginal in the global H_2 cycle and relatively diffuse, it remains that large industrial H_2 deposits may well have been formed by the accumulation of gaseous H_2 at small rates (hundreds of kg $H_2.yr^{-1}$) over geological timescales (Ma). To date, such accumulations have not yet been reported. The fact that H_2 can be produced in the laboratory under geologically relevant P-T conditions for weeks or months from natural rock samples (e.g., Seyfried et al., 2007; Marcaillou et al., 2011; McCollom and Donaldson, 2016; Miller et al., 2017; Huang et al., 2017, 2019, 2023) raises the question of its possible renewable nature. If, for a small H_2 accumulation (e.g., H_2 in karst cavities, Maiga et al., 2023), the recharge rate is commensurable with the economic production of a well, operating a well drilled in this small accumulation may turn profitable and H_2 could then be considered renewable from an industrial point of view.

3 Economic constraints on natural H_2 accumulation volume and renewable flux

In this section, minimum H_2 accumulation volume and renewable flow-rates are estimated based on the minimum amount of H_2 that must be produced from a single well for its operation to be profitable. Only high-purity H_2 accumulations, as in Bourakebougou (Mali), will be considered in order to avoid estimating gas purification costs in the case of diluted H_2 (e.g., in N_2). Drilling costs represent about 2/3 of the total drilling operations, including preparation and completion, which themselves represent about 40 % of the total exploration and development costs (Hossain, 2015). Drilling costs are highly dependent on the depth of the well (Table 1). For simplicity, they are estimated based on two scenarios, (i) a shallow accumulation as in Bourakebougou and (ii) a deep one, which requires drilling down to 200 and 3,000 m, respectively. To be competitive, we estimate the maximum price of H_2 at the well exit (before treatment and transport) at a maximum of €1/kg. Indeed, €1/kg is the target cost for decarbonised H_2 (Wu et al., 2022) or 'blue hydrogen', which is produced from methane but with CO_2 capture and storage. Gas pressure is estimated to 20 bar at 200 m and 300 bar at 3000 m. In the best case (100 % recovery and 100 % exploration success rate), 2 and 10 kt H_2 must be recovered per well, respectively, before the industrial project becomes profitable.

Considering typical reservoir characteristics (Table 1), a minimum reservoir size can be assigned to the hydrogen mass to be recovered for each well depth (200 and 3000 m). A recovery factor of 0.8 and a reservoir thickness of 25 m, typical for gas reservoirs, are considered (Table 1). The mass/volume conversion factor for H_2 is 11 m^3/kg under surface conditions. Applied to the Mali example (Scenario 1) where 25 wells have been drilled (Maiga et al., 2023), the equivalent reservoir surface would be of ca. 9 x 10^6 m^2, i.e., a 25 x 600 m x 600 m surface (Table 1). Due to geological risk, a success ratio for exploration drilling must be taken into account for a more realistic minimum estimate of profitable H_2 production. In oil and gas exploration, a discovery is made on average every five to ten wells (Levitt, 2016), and this discovery must finance the unsuccessful wells. We will consider here a success rate of 20 % which is fairly optimistic given that H_2 systems are far less known than the oil and gas systems. Therefore, we consider that five times more H_2 must be recovered, corresponding to 10 and 50 kt, for the 200 m and the 3000 m drilling scenario. Converted into gaseous H_2 reservoir size, a reservoir volume of 45 x 10^6 m^3 (1350 m x 1350 m x 25 m) is obtained for the shallow well example and 2.5 x 10^6 m^3 (300 m x 300 m x 25 m) for the deep well example.

Table 1. Well costs and minimum hydrogen volume for ROI with associated reservoir surface and volume based on €1/kg H_2.

Well depth (m)	200	3000
Well cost (€)	2×10^6	1×10^7
H_2 mass equivalent (kg)	2×10^6	1×10^7
H_2 vol. equivalent (sm^3)	2.2×10^7	1.1×10^8
H_2 vol. eq. at depth (m^3)	1.1×10^6	3.67×10^5
Recovery factor	0.8	0.8
Porosity (%)	15	10
Reservoir thickness (m)	25	25
Host-rock volume (m^3)	9.2×10^6	4.6×10^5
Reservoir surface (m^2)	3.7×10^5	1.8×10^4
Equivalent-square side (m)	606	135

So far, no such large H_2 gas accumulation has been reported, however, rapid gas recharge upon extraction has been claimed at Bourakebougou (Maiga et al., 2023) as in the case of Lorraine (France) where, however, H_2 is only present as dissolved species in an aquifer (Fontecave et al., 2024) and not as a free gas phase. Based on a return on investment of 5 and 3 years, the H_2 extraction rate should be on the order of 2 to 3 and 10 to 17 $kt.yr^{-1}$, respectively, to cover the drilling expenses. This extraction rate can be seen as a rough estimate of the rate of recharge of the H_2 gas accumulation for H_2 to be considered renewable from an economic point of view.

The question now is whether small accumulations with a short H_2 residence time can meet the economic requirements estimated above. Basically, the rate of natural processes of H_2 production, consumption and transport must compare to the economic recharge rates described above. This question is addressed here through the simulation of H_2 fluxes in a simplified H_2 system where the recharge process is the degassing in an aquifer of H_2 produced deeper in the course of water-rock interactions. Such a setting is similar to what is described both in Mali (Maiga et al., 2023) and in Kansas (Guélard et al., 2017) where degassing depths are 800 m and ca. 300–400 m, respectively.

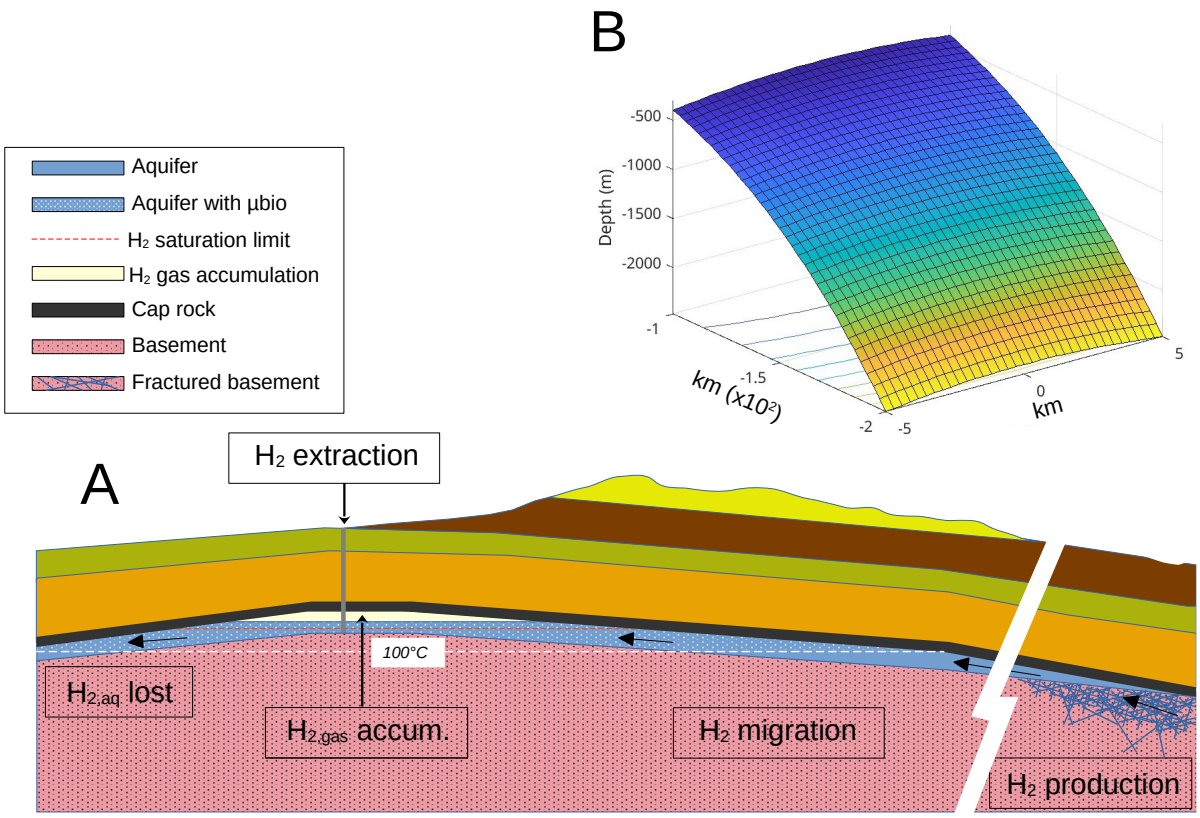

Figure 2. Conceptual model of H_2 production, transport and accumulation designed to constrained H_2 accumulation rates in the context of a deep aquifer. (A) Section through the aquifer highlighting the source, transport and accumulation zones where H_2 will be extracted. H_2 is produced by water – ultramafic rock interaction. H_2 migrates as free gas and/or dissolved species (at the same rates) in the aquifer water and can potentially accumulate at the top of the aquifer as a gas phase. In the model, H_2 degassing may occur upon migration towards the surface if H_2 saturation is reached. Aqueous H_2 can be consumed by microbial activity at temperatures below 100 °C. Beyond the H_2 accumulation zone, remaining dissolved H_2 is basically lost to the system. (B) Roof surface of the H_2 catchment volume of the aquifer considered of pseudo-parallelepiped geometry to simplify H_2 volumetric flux calculation.

4 Simulation of H_2 gas accumulation rates in a deep aquifer setting

4.1 Aquifer model geometry

A conceptual 1-D model (Figure 2 and S3, Table 2) is developed in order to simulate H_2 production, transport and accumulation in a deep aquifer. As mentioned earlier, studies in Mali and Kansas where H_2 gas concentration and pressure have been measured in wells both suggest H_2 stored in an aquifer. In the present model, H_2 is produced by interaction between the aquifer water and host rocks (Production Zone, PZ). Subsequently, H_2 is transported either as dissolved gas or both as a free and a dissolved gas phase in mutual equilibrium, towards the surface at a rate corresponding to the aquifer flow-rate which is taken as constant. As long as H_2 is present, we consider that it can be consumed by microorganisms only at temperatures below 100 °C (Figure S3) according to a thermally deactivated process, i.e., at a rate which decreases with T. The H_2 solubility – depth relationship within the aquifer is derived from Lopez-Lazaro et al. (2019) considering a geothermal gradient of 30 °C/km , hydrostatic pressure and a salinity of NaCl ~ 0.6 M (not considered in the thermochemical calculations).

At the Accumulation Zone level, H_2 gas, if any, accumulates whereas dissolved H_2 is further transported in the flowing aquifer and will not accumulate (Figure 2A and S3). The accumulation rate is then compared to an economical H_2 flux defined as the minimum exploitation flux that must be recovered for the drilling and completion infrastructure costs to be amortised within 3 or 5 years. This conceptual model is aimed at evaluating the magnitude of the main H_2 production and consumption fluxes. In order, to translate 1-D flux in mole $H_2.m^{-2}.yr^{-1}$ into H_2 volumes in $m^3.yr^{-1}$ a simplified aquifer 3-D geometry was adopted (Figure 2B).

4.2 Production Zone

The production zone in the aquifer is the locus of water-rock interactions which lead to H_2 production. The present conceptual model requires gas saturation in order for H_2 to accumulate. Based on their relevance according to literature, four H_2 producing reactions have been considered along with radiolysis, which involve the following set of phases, siderite/magnetite, hematite/magnetite and olivine along with its serpentinisation products. Deep-seated H_2 from Earth's core/mantle degassing (Zgonnik, 2020; Zhu et al., 2025) may contribute to the H_2 budget of the aquifer; the magnitude of this contribution cannot be assessed in the present state of knowledge and this process has therefore been ignored here. Similarly, in the case of serpentinisation, the release of H_2 hosted as fluid inclusion in olivine has not been considered. Indeed, although this type of inclusions may contain H_2, they have be mainly studied for their CH_4 content (Klein et al., 2019).

Natural H_2 production by radiolysis has been invoked for its potential to fuel deep surface microbial communities (Lin et al., 2005a,b). Uranium, Th and K decay in rocks produces ionising radiation. The generated α, β and γ particles split water into $e^-_{(aq)}$, $HO\cdot$, $H\cdot$, $HO_2\cdot$, H_3O^+, OH^-, H_2O_2 and H_2 (Le Caër, 2011). The model of Aitken (1985) and Hofmann (1992) is usually used to predict H_2 production in rocks (Lin et al., 2005b; Bouquet et al., 2017). In this model, ionising radiations generated in the rock induce water radiolysis in the pore water. The calculation of the steady-state concentration of radiolytic H_2 with depth along a one dimensional z profile is detailed in Supplementary Material. It involves as sink terms, the vertical H_2 transfer to the surface by Fickian diffusion and the H_2 consumption through the reaction:

$$H_{2,aq} + 1/2\ O_{2,aq} = H_2O \qquad (1)$$

among radiolytic products. The kinetics of Reaction (1) is taken from Foustoukos et al. (2011), but with a pre-exponential factor A = 0.15 s^{-1} instead of the value provided in the original publication (correction confirmed by D. I. Foustoukos). Fig. 3 shows how the role of Reaction (1) on the calculation of the steady-state radiolytic H_2 concentration is paramount. Aqueous H_2 concentrations below 10^{-2} nM are expected at depth in a steady state regime.

Similarly, H_2 flux at the surface can be calculated (through Equation S5) with and without considering Reaction (1). Hydrogen surface fluxes are 5 orders of magnitude lower when Reaction (1) is not considered (see Suppl. Material). Using the estimated surface area of Precambrian terranes (1.06×10^8 km^2) from Lollar et al. (2014) leads to a global H_2 flux for 1 % of porosity of 6×10^{10} $mol.yr^{-1}$ when considering radiolysis, in agreement with the estimates of Lollar et al. (2014). When considering H_2 consumption, the global H_2 flux is of 8×10^4 $mol.yr^{-1}$(160 $kg.yr^{-1}$), that is five to six orders of magnitude lower than the main processes known to produce H_2 in geological environments (Lollar et al., 2014). Since net H_2 production through radiolysis decreases with depth, H_2 fluxes at the basis of an aquifer will be lower than the surface flux (i.e., ca. 600 mol. H_2 $km^{-2}.yr^{-1}$ or, more realistically, 0.7 mmol H_2 $km^{-2}.yr^{-1}$ if H_2 reaction with O_2 is considered). Gaseous H_2 saturation will not be achieved in our modeled aquifer with a radiolytic H_2 source.

Comparatively, H_2 production through RedOx reactions has a higher potential to reach H_2 gas saturation in a deep aquifer. The decomposition of siderite has been proposed as a possible source of natural H_2 by interaction with water (Milesi et al., 2016; Malvoisin and Brunet, 2023). In the presence of water, either vapor or liquid, siderite produces H_2 and CO_2 as volatile species (McCollom, 2003; Milesi et al., 2015) according to the reaction:

$$\underset{\text{siderite}}{3\,FeCO_3} + H_2O = \underset{\text{magnetite}}{Fe_3O_4} + 3\,CO_2 + H_2 \qquad (2)$$

Note that under equilibrium both reactants and products are stable and the H_2 and CO_2 activities are related through the equilibrium constant of Reaction (2) which is a function of T and P. Assuming a closed chemical system where siderite reacts with an H_2- and CO_2-free water then $[CO_2]$ = 3 $[H_2]$, i.e., 3 moles CO_2 together with 1 mole H_2 are produced according to that reaction as long as the saturation in one of these two gases is not achieved.The formation of CH_4 from CO_2 + H_2 under aqueous conditions is neglected for kinetic reasons (McCollom and Donaldson, 2016). Under these circumstances, $[H_2]$ can be calculated as a function of T, P or as a function of depth knowing the geothermal gradient (Figure 4). It can be seen on Figure 4 that even if siderite – water interaction occurs at depth as high as 7,000 m, H_2 gas saturation is not expected to be achieved upon $H_{2,aq}$ migration towards the surface. H_2 saturation may become possible if the CO_2 concentration at the production zone is lowered by several orders of magnitude thanks to an independent process. It is worth noting that $[H_2]$ here is independent from the amount of siderite available as long as it is in excess. Given the low potential of siderite-water interaction to enable H_2 gas saturation in the aquifer, this H_2-producing reaction will not be considered further.

RedOx reactions involving magnetite oxidation have also been reported in the literature which have been invoked for the production of H_2 from banded iron formations (BIF) that can be abundant in cratonic settings (Geymond et al., 2022). The H_2 activity calculated considering magnetite – hematite equilibrium:

$$\underset{\text{magnetite}}{2\ Fe_3O_4} + H_2O = \underset{\text{hematite}}{3\,Fe_2O_3} + H_2 \qquad (3)$$

is far too small for H_2 gas saturation to be reached (Fig. 4), therefore, Reaction (3) will not be examined further. Recent experimental data suggest that the adjustment of magnetite stoichiometry during interaction with water could be a source of H_2 (Geymond et al., 2023). However, by lack of thermochemical description of the proposed H_2 produc-

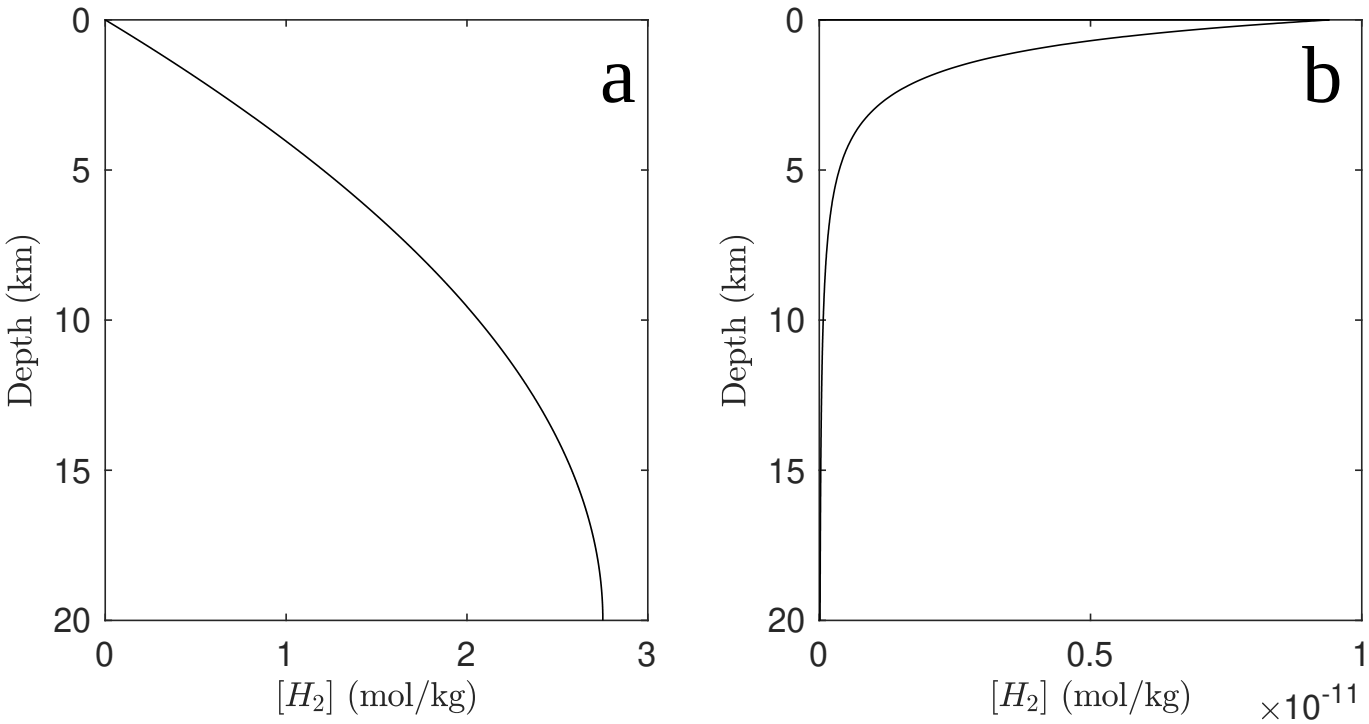

Figure 3. Calculated H_2 concentration (lines) as a function of depth for the steady-state diffusion model when considering radiolysis only (a), and both radiolysis and H_2 consumption through chemical reaction with radiolytic O_2 (b). Porosity is set to 1 %.

tion mechanism, the corresponding experimental results cannot be transposed to natural settings and could not be considered here.

The reaction between olivine and water produces serpentine, brucite, magnetite and H_2 at temperatures below 340 °C (in the pressure range of interest for the present study), according to a reaction known as olivine serpentinisation, which can be simplified as follows:

$$30\,\underset{\text{olivine}}{(Mg_{0.9}Fe_{0.1})_2SiO_4} + 41\,\underset{\text{water}}{H_2O} = 15\,\underset{\text{serpentine}}{Mg_3Si_2O_5(OH)_4} + 9\,\underset{\text{brucite}}{Mg(OH)_2} + 2\,\underset{\text{magnetite}}{Fe_3O_4} + 2\,H_2 \quad (4)$$

Reaction (4) neglects the possible incorporation of iron in both serpentine and brucite. For a given starting olivine composition, the amount of H_2 that can be produced depends on the iron content of these two minerals. Mg/(Fe+Mg) ratio (Mg#) in serpentine from oceanic samples varies typically from 0.92 and 0.99 (Mayhew and Ellison, 2020) whereas Mg# in natural brucite can reach values as low as 0.6 (Beard and Frost, 2017) with an average value around 0.8 (Klein et al., 2014). Iron in serpentinite can be present both as Fe^{2+} and Fe^{3+} (Beard and Frost, 2017) with an $Fe^{3+}/\sum Fe$ ratio which will depend on the H_2 activity, a_{H_2}. Awaruite, Ni_3Fe, is a common accessory mineral in serpentinite (Dick, 1974; Schwarzenbach et al., 2021) which is stabilised at high a_{H_2}. Awaruite must be considered when dealing with RedOx equilibria in serpentinite. RedOx equilibria such as Reaction (5) can be written between awaruite, serpentine and brucite.

$$[Mg_3Si_2O_5(OH)_4]^{\text{serpentine}} + Ni_3Fe + 8\,H_2O = [Ni_3Si_2O_5(OH)_4]^{\text{serpentine}} + 3\,[Mg(OH)_2]^{\text{brucite}} + [Fe(OH)_2]^{\text{brucite}} + 4\,H_2 \quad (5)$$

Ni is an ubiquitous minor element in olivine which can also be incorporated in serpentine as a nepouite component, $Ni_3Si_2O_5(OH)_4$.

The $[H_{2,aq}]$ in equilibrium with the serpentinisation products of olivine + orthopyroxene (synthetic harzburgite) was calculated using Perple_X along the chosen geothermal gradient and plotted as a function of depth on Figure 4. For both olivine and pyroxene an Mg/(Mg+Fe) ratio of 0.91 was used. Ni was added to olivine considering a Ni/(Ni + Fe + Mg) ratio of 0.004 (see Suppl. Material). Simplified harzburgitic mineralogy was 65 mol.% olivine + 35 mol.% orthopyroxene. The synthetic rock was reacted with pure water in a water-to-rock mass ratio of 0.2 which is (1) slightly above the minimum water-to-rock ratio (0.18) below which water is the limiting reactant to complete olivine hydration and (2) corresponds to a porosity of ca. 6 % in the ideal case where water in chemical equilibrium with the whole rock, which is close to the porosity used in the model. Therefore, the equilibrium $[H_2]$ calculated with a water-to-rock mass ratio of 0.2 in a closed system represents an upper bound of $[H_2]$ expected in the H_2 source zone of the aquifer where apparent water-to-rock mass ratios will be higher than 0.02. Serpentinisation products are composed of serpentine ± brucite ± magnetite ± awaruite. Serpentine (lizardite) is considered as a solid solution comprising Fe^{2+}, Mg^{2+},

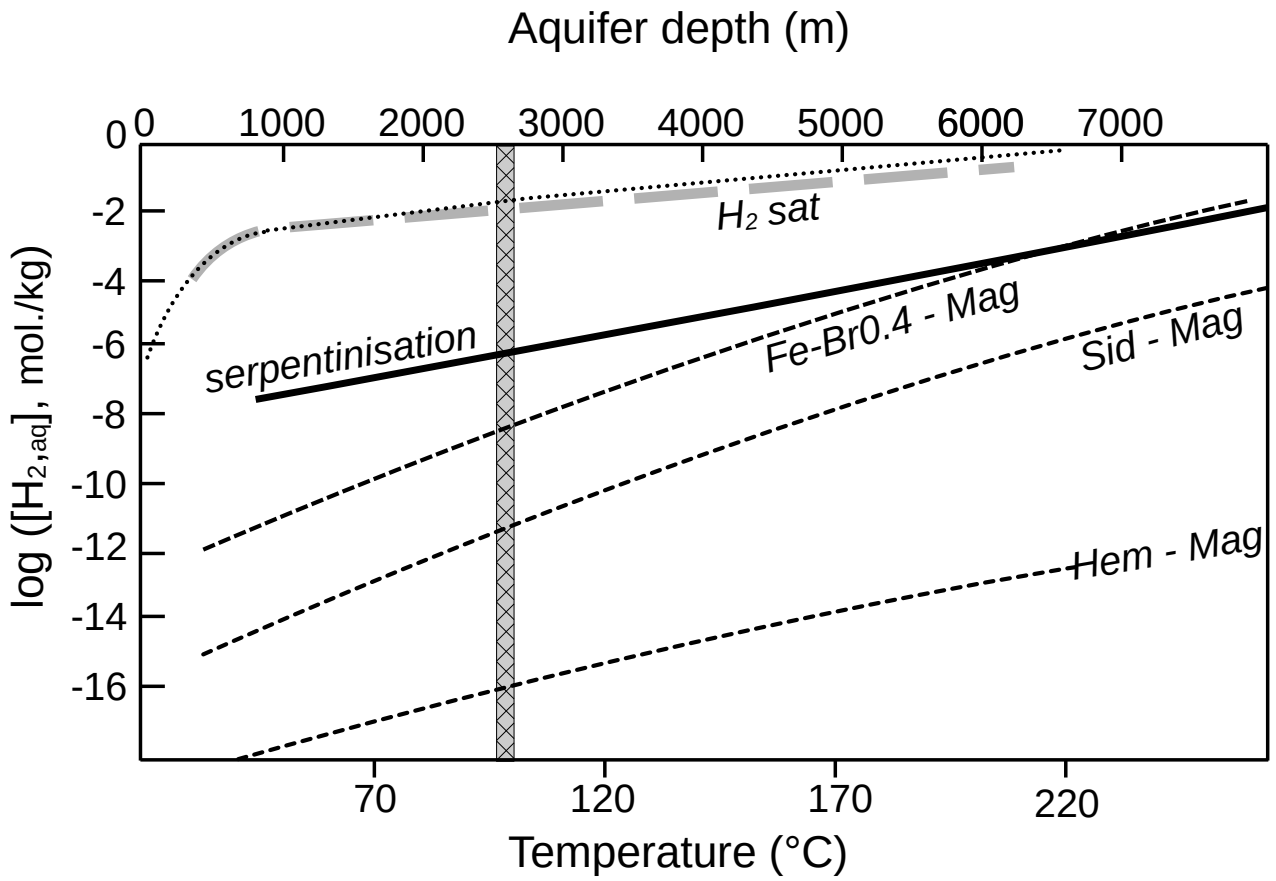

Figure 4. Natural logarithm of the H_2 concentration produced by the serpentinisation of a Ni-bearing harzburgite with pure water as a function of depth. H_2 concentration in equilibrium with siderite-magnetite, hematite-magnetite and Fe-brucite (xFe = 0.4)-magnetite are plotted for comparison. Serpentinisation reaction is model with Perple_X (see Suppl. Material) whereas all the other equilibria are calculated with SUPCRT (slop98 database, Johnson et al., 1992). A geothermal gradient of 30 °C/km is used assuming hydrostatic pressure. H_2 gas saturation curves calculated from SUPCRT (dotted line) and used in the present model (thick grayish dashed line, Lopez-Lazaro et al., 2019) are plotted for comparison. The vertical line with crosses represents the limit of microbial life considered in the model (100 °C isotherm). No gas phase other than H_2 is considered to occur at depths greater than H_2 gas saturation depth (in water). A free gas phase (e.g., N_2) present at greater depth would incorporate an H_2 component (Henry's law) which however would result in low-grade H_2 gas (case not considered here). The P-T conditions studied here are below the H_2-H_2O critical curve (Seward and Franck, 1981).

Fe^{3+} and Ni end-members. The thermochemical properties of the serpentine ferric end-member, $Fe^{3+}{}_2\square Si_2O_5(OH)_4$ and those of nepouite have been estimated, (see Suppl. Material). Brucite solid-solution is considered as ideal and the thermochemical properties of $Fe(OH)_2$ end-member, amakinite, are taken from Carlin et al. (2024) who revisited the database of McCollom and Bach (2009). The Fe-brucite-magnetite RedOx equilibrium studied by Carlin et al. (2024) is also plotted on Fig. 4 for an Fe-rich brucite composition, $(Mg_{0.6}Fe_{0.4})(OH)_2$. Perple_X output indicates that equilibrium $[H_2]$ is controlled by RedOx equilibria involving both iron and nickel at the serpentinisation conditions used in the calculation (see Suppl. Material).

Figure 4 shows that among the H_2-producing reactions reviewed here, serpentinisation of ultramafic rocks appears to be the only one that makes it possible to achieve H_2 gas saturation in the water rising in an aquifer. Serpentinisation is therefore chosen as the H_2 production reaction in the present H_2 production/transfer/accumulation model. A deep source (> 5,000–6,000 m) is required and saturation will only occur at depths of less than 2,500 m, i.e., for T below 100 °C. The ultramafic source rocks are considered as located in the sedimentary basin bedrock (Fig. 2A). They

interact with the aquifer water through a fractures network described, in the model, by an equivalent porosity factor (K, see Suppl. Material).

Dihydrogen production kinetics in the course of serpentinisation were modelled based on olivine reactivity (i.e., neglecting thereby the role of orthopyroxene as H_2 source). The proportion of olivine in the initial rock can be adjusted in order to simulate H_2 production from an ultramafic rock that is already partially serpentinised. A zero-order kinetics is used with a dependence in both temperature and olivine surface area, which was taken from the data compilation found in Carlin et al. (2024, their Fig. 3B). The choice of a zero-order kinetics is a simplification which does not account for the evolution of mineral product compositions and thus the evolution, with reaction progress, of the number of H_2 mole produced per olivine mole. The olivine surface area evolution with reaction progress was considered as constant so that the rate of H_2 production writes:

$$\frac{d[H_2](T)}{dt} = ks.SA^0{}_{Ol/liter} = ks^0.exp(\frac{-E_a}{RT}).SA^0{}_{Ol/liter} \quad (6)$$

where ks is the dissolution kinetics constant in mole H_2 per olivine surface area (m^{-2}) per year which is thermally activated with ks^0, the pre-exponential factor and Ea, the activation energy. $SA°_{Ol/liter}$ is the initial olivine surface area is calculated using the relationship provided in Brantley and Mellott (2000) and expressed in m^2 per m^3 of water in the aquifer. In the present model, two $H_{2,aq}$ concentration thresholds cannot be exceeded at the source zone: (1) $[H_{2,aq}]$ at H_2-gas saturation and (2) $[H_{2,aq}]$ imposed by Reaction (5) for a given Ni content of the reacting olivine (see Suppl. Material), noted $[H_{2,aq}]_{max}$, at the P and T conditions of the Production Zone. In practice, threshold (1), i.e., H_2 gas saturation, cannot be reached in the Production Zone, except under near-ambient conditions (i.e., subsurface Production Zone, Fig. 4) where both kinetics and thermochemical extrapolation are however uncertain.

If concentration threshold (1) is attained, the H_2 production kinetics is controlled by the rate of H_2 flushing by the aquifer in order to maintain constant $[H_2] = [H_{2,aq}]_{max}$. Once olivine is exhausted, H_2 is no longer produced by olivine serpentinisation, but the mineral products of Reaction (5) can still produce H_2 through their chemical interation with the aquifer water as shown by Carlin et al. (2024) for the oxidation of the $Fe(OH)_2$ component of brucite into magnetite. At a later stage, the olivine serpentinisation products can no longer maintain $[H_{2,aq}]_{max}$, $[H_{2,aq}]$ starts decreasing and, to a certain extent, awaruite will be consumed, brucite Mg# and Fe^{3+} content in serpentine will increase. The maximum H_2 source production lifetime (*life*) is defined as the maximum duration of H_2 production process under steady state conditions, i.e., constant H_2 concentration. To calculate the *life* parameter, a yield of H_2 must be assigned per mole of reacted olivine. Maximum yield will be taken here which is achieved for complete oxidation of the ferrous iron contained in the starting olivine. Considering a starting olivine of Fo_{91} composition, at best, 0.09 mole of H_2 can be produced, i.e., 11 moles of olivine per mole H_2.

From Relation (6), the steady-state H_2 concentration at x = 0, $[H_2]_{x_0}$, i.e., at the outflow of the Production Zone (Figure 2) writes:

$$[H_2]_{x_0} = \frac{d[H_2]}{dt}.\frac{L_{PZ}}{U} \qquad if\ [H_{2,aq}] \leq [H_{2,aq}]_{max} \quad (7)$$

where L_{PZ} is the length (1D) of production zone (m) and U the aquifer flow rate L_{PZ}/U is thus the duration of renewal (y) of the aquifer water in the PZ. Otherwise,

$$[H_2]_{x_0} = [H_{2,aq}]_{max} \quad (8)$$

5 H_2 consumption rates by microbial activity

We showed above (Figure 4) that H_2 gas saturation in the aquifer and, thus, possibly, H_2 gas accumulation, are possible if and only if H_2 is produced at depths $>$ 5,000 m, i.e., for Production Zones located at depths greater than ca. 5,000 m. If gas saturation is achieved, both gas and aqueous H_2 are assumed to migrate at the aquifer flow-rate. The water temperature to be considered for Production Zones at such depths are always above the temperature threshold for microbial growth defined here as 100 °C. Thus, H_2 is first transported isochemically across the abiotic zone (Figure S4), until it reaches a zone where it can be partly or fully consumed by microbial activity (BioZone). Microbial activity is considered to operate in aqueous medium mainly. However, it will be considered that H_2 dissolution is fast relative to microbial consumption and is not the rate limiting factor. In other words, H_2 concentration in the aquifer is the saturation concentration as long as H_2 gas is present even in the presence of microbial activity.

The dynamics of microbial biomass as a function of substrate concentration can be accounted for by a Monod-type kinetic law. A rigorous biotic H_2-consumption model would use this type of kinetics along with the cell-specific hydrogen consumption for each terminal electron-accepting process (Thaysen et al., 2021) and the number of cells present over time. Under steady-state biomass conditions which applied in the present study, the substrate (H_2) consumption is often showed to follow a Michaelis-Menten law (Robinson and Tiedje, 1984; Häring and Conrad, 1994; Dong and Layzell, 2001; Constant et al., 2008; Greening et al., 2015; Myagkiy et al., 2020) which writes in its differential form as:

$$\frac{d[H_2]}{dt} = -V_m \frac{[H_2(t)]}{K_m + [H_2(t)]} \quad (9)$$

where V_m is the consumption rate (mole per volume unit and time unit) at substrate saturation and K_m, the half-

saturation concentration constant. As long as H_2 saturation is not achieved (i.e., $x \leq x_{sat}$), $[H_2](x)$ is calculated by numerical integration of Equation (9) where V_m is a function of x (see below) and K_m a constant.

Rates of H_2 consumption in aqueous media by microorganisms in the presence or absence of sediments have been measured in laboratory incubation. A survey of experimental data is given in Thaysen et al. (2021) for homoacetogenesis, methanogenesis and sulfate reduction. Laboratory consumption rates typically vary between 1 and 100 $\mu M.h^{-1}$. More recently, Dohrmann and Krüger (2023) sampled native fluids from a gas field (2,700–3,500 m) and incubated them under pressure (100 bar) and temperature (30 and 60 °C) with H_2 (10% in N_2). Consumption rates in the order of 10 $\mu M.h^{-1}$ (30 °C) were found which decreased by more than one order of magnitude at 60 °C.

Incubation experiments on Cape Cod aquifer slurry (Harris et al., 2007), yielded Michaelis-Menten kinetics with V_m in the order of 10 $pM.h^{-1}$ and a K_m of 0.16 pM. Average K_m values for 4 methanogens and 5 sulfate-reducing strains were found to be 6 and 1.5 pM, respectively (Robinson and Tiedje, 1984). Similarly, K_m of 6 pM was found for a H_2-oxidising CO_2-reducing acetogenic bacteria isolated from termite gut (Breznak and Switzer, 1986). We therefore propose to test two H_2-consumption cases, with a high Michaelis-Menten kinetics (*fast*) at 25 °C with V_m^f = 100 $pM.h^{-1}$ and K_m^f = 1 pM and a low kinetics one (*slow*) with V_m^s = 1 $pM.h^{-1}$ and $K_m^s = K_m^f$ = 1 pM. In order to account for the lowering of the H_2 consumption rate observed by Dohrmann and Krüger (2023), we applied a deactivation energy (E_d = -110 kJ/mol) on V_m in the form:

$$V_m = V^0{}_m . exp(-\frac{E_d}{RT}) \quad (10)$$

with $V_m^{0,f}$= 1.38 × 10^{-17} $pM.h^{-1}$ and $V_m^{0,s}$ = 1.38 × 10^{-19} $pM.h^{-1}$ with T in K.

6 Results and Discussion

On the basis of thermochemical considerations, we show that among H_2-producing reactions based on the oxidation of ferrous iron contained in rock-forming minerals to ferric iron, (olivine) serpentinisation is the only one capable of achieving H_2-gas saturation in an up-ward flowing aquifer. Aquifer degassing can proceed at depths < 2,500 m, i.e., in a range of temperatures where microbial life is possible and, thus, where aquifer H_2 can at least be partly consumed (Fig. 4). We confirm thereby the potential already noted for serpentinisation to generate a 'hydrogen system' (Lefeuvre et al., 2021; Jackson et al., 2024). As shown in Figure 4, however, H_2 gas saturation in an aquifer can only be achieved if H_2 is generated at depths of more than 5,000 m or under near-surface conditions (< ca. 100 °C). H_2 gas saturation in the Production Zone can only be achieved under near-surface conditions, which may apply to the case of H_2 bubbling in alkaline springs from ophiolites (e.g., Vacquand et al., 2018; Leong et al., 2023; Corre et al., 2023). Under these conditions, $[H_{2,aq}]$ is small (10^{-3}–10^{-2} mole/kg) and therefore corresponding degassing fluxes are relatively small as well.

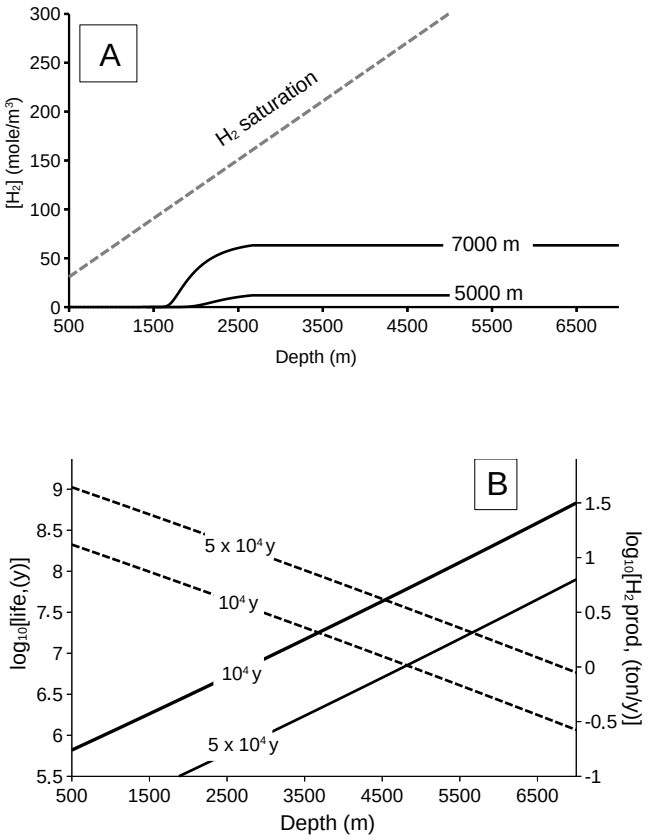

Figure 5. Model output. (A) H_2 concentration profile for a deep source (5,000 and 7,000 m) where olivine serpentinisation takes place. Source concentration equals $[H_{2,aq}]^{max}$ which is a function of temperature and thus depth. H_2 is transported with the same concentration towards the BioZone where it is fully consumed assuming the lowest of the two H_2 consumption kinetics (V_m^s and K_m) used in the model. Gas saturation (dashed line) is never reached and then gas accumulation is not triggered. Aquifer flow-rate is 5 $m.yr^{-1}$. (B) Source (7,000 m) production characteristics for two water renewal times (*see* text), 10^4 and 5 x 10^4 years. For an aquifer cross-section of 1 km^2 and a porosity of 0.05, H_2 production rates at the source equals a few tens of tons per year. H_2 production under steady-state conditions lasts around 1 Ma. Dotted line = source lifetime; solid line = source prod.

The potential of serpentinisation to yield H_2 accumulation at the several of $kt.yr^{-1}$ level, i.e., compatible with a renewable resource for an industrial-scale exploitation, in a deep aquifer setting was further modeled with the aquifer and production zone parameters summarised in Table 2. The key parameter that will constrain the H_2 flux in the aquifer is the ratio between 1D PZ length and aquifer flow-rate which corresponds to the characteristic time of water

renewal in the PZ. H_2 production has been simulated for Production Zones (PZ) located at depths from 5,000 m and up to 7,000 m, corresponding to temperatures from 170 to 230 °C, respectively, according to the average continental geothermal gradient chosen here (Table 2).

The highest [H_2] that can be reached in a production zone at 7,000 m, which will generate the highest H_2 flux in the aquifer for a given aquifer flow-rate, is $[H_{2,aq}]_{max}$. It is achieved for water renewal times above 10^3–10^4 year (Figure S5). This corresponds to a 1D production-zone of around 10 km long for an aquifer flow-rate of 1 m.yr^{-1}.

The calculation of H_2 accumulation rates (mole.yr^{-1}) from the 1D model requires defining the aquifer cross-section through which passing H_2 is accumulated. For that purpose, a H_2 catchment zone is defined having a width of 10 km (Fig. 2B). The relevant aquifer section to calculate H_2 accumulation rates is then 1 km^2 (10 km x 0.1 km aquifer thickness). The corresponding cross-section of fractured ultramafic rock through which water flows to promote serpentinisation is obviously much larger depending on the fracture density that is considered (see K factor, Suppl. Material).

Two sets of Michaelis-Menten constants (*fast* and *slow*) were used to model H_2 microbial consumption and to retrieve H_2 gas accumulation rate, if any, for a given production zone depth. Accumulation depth was set to 200 m in accordance with the scenario used to evaluate drilling costs. These costs were also estimated for a 3,000 m accumulation. However, it can be readily seen on Figure 4 that saturation is not achieved at 3,000 m when considering serpentinisation and therefore gas accumulation by aquifer degassing is not possible in that case.

The microbial H_2 consumption is found to represent a strong filter which prevents large accumulation rates at shallow depth (200 m here). Simulation in the case of a renewal time of 50,000 year (PZ_{length} = 50 km and *flowrate* = 1 m.yr^{-1}, Figure 5A) and 10,000 year (PZ_{length} = 50 km and (*life*) is defined as the maximum duration of H_2 production process under steady state conditions, i.e., constant H_2 concentration. To calculate the *flowrate* = 5 m.yr^{-1}) with source depths of 5,000 and 7,000 m (aquifer dip = 2°) shows that all H_2 is consumed by the microbial life and that H_2 gas saturation cannot be achieved in the aquifer. For this simulation, the microbial consumption rate is set to its smallest value (V_m^s), it must be lowered by three orders of magnitude for H_2 accumulation at 200 m to become possible. In that case, around half of the source production can be recovered in the form of accumulated H_2. The H_2 concentration constraint at the source ($< [H_{2,aq}]_{max}$) limits the H_2 source flux (mole.m^{-2}.yr^{-1}). For a 1 km^2 aquifer cross-section, source production rate is of a few tens of tons per year (Figure 5B) at most, considering realistic aquifer flow-rates in the 0.5 to 5 m.yr^{-1} range (e.g., Wei et al., 1990; Janetz et al., 2020; Kamdee et al., 2022). Due to the concentration limitation at the Production Zone, even if H_2 could be transported without loss (consumption/leakage), accumulation rates would not exceed the source production rate of a few tens of ton.yr^{-1} and H_2 will not be renewable according to the economical criteria defined here. Increasing the PZ_{length} cannot lead to higher H_2 accumulation rates since $H_{2,aq}$ concentration is limited, it only increases the H_2 source lifetime. Typical source lifetime can be estimated from the model to about 1 Ma for aquifer water renewal time of 10^4 years (Figure 5B). Small accumulation rates ($<$ ca. ton H_2 per year) by H_2 degassing at shallow levels ($<$ 500 m) over a long time (Ma) is possible with a deep-seated serpentinisation source ($>$ 7,000 m) provided that source temperature remains below 350–375 °C, the temperature range above which olivine + H_2O is stable. In any case, regardless of the H_2 transport, consumption and saturation parameters used to model the current idealised aquifer, renewability is ruled out by the estimated magnitude of H_2 source flux (i.e., in the Production Zone) which is tightly constrained by thermodynamics and aquifer flow-rate. However, the model shows that significant accumulation of H_2 gas can proceed over time. The corresponding accumulation characteritics will directly depend on (1) the Production Zone parameters. The effect of the Production Zone geometry is relatively straightforward since it will directly affect the H_2 production potential and flux (mole H_2 and mole H_2/y) and thus the volume of the accumulation, if any. The mineralogy of the source rock is probably the most critical parameter. The occurrence of ultramafic rocks in cratonic setting has been widely documented and their volume has even been estimated (Lollar et al., 2014). Recently, the distribution of proterozoic ophiolites in the Arabian Nubian shield has been used as a guide for H_2 exploration (Saidy et al., 2024). On the other hand, the H_2 fertility of these ancient ophiolites is unclear. Although primary olivine is sometimes described, they are often strongly serpentinised (e.g., Zimmer et al., 1995; Ahmed et al., 2001; Shahien et al., 2021). In the present model, the amount of primary olivine has been set to 20 wt% in order to account for previous serpentinisation, but this figure may well be too high in most cases. The accumulation characteristics will also drastically depend on (2) the microbial consumption in the aquifer. Direct application of the rare H_2-consumption data that are available indicates that micro-organisms should basically consume all H_2 produced abiotically by water-rock interactions. The transposition of laboratory data (and the few in situ measurements in aquifers) must be treated with caution since specific environmental conditions may lead to different consumption behaviours. Owing to the prominent role of biological activity, the contact time between H_2 and consumers in the aquifer is an important parameter related to H_2 transport (mean and rate). The present model considers that H_2, even as a gas phase, migrates at the aquifer flow rate. However, in a two-phase flow model, it is generally considered that gas migrates at higher rate than water. In this case, higher H_2 gas accumulation rates will be achieved. The fast migration of a large gas volume, possibly through a fractures network (not considered in the model), may also limit the magnitude of the H_2 consumption by micro-organisms. Finally, another important parameter which has not been considered here and that will control the H_2 accumulation volume dynamically is (3) the H_2 leakage

Table 2. Aquifer and H_2-source main characteristics used in H_2-gas flux modeling. Additional information are found in the text body. PZ stands for Production Zone.

Thickness (m)	100	Flow rate ($m.yr^{-1}$)	0.5–5
Dip (°)	2 and 5	$[Olivine]_{rock}$ in PZ (wt%)	20
Porosity (%)	5	Accum. Zone depth (m)	200
Width H_2 catchment (km)	10	Geothermal gradient (°C/km)	30
Prod. Zone thickness (m)	100	Surface temperature (°C)	20
Olivine radius (µm)	200		

rate (Prinzhofer and Cacas-Stentz, 2023) which may occur to be higher than the accumulation rate.

7 Conclusions

Exploration of 'white hydrogen' is developing rapidly, driven by the need to gradually replace fossil fuels. Current basic research and R&D efforts should enable us to assess the potential role of 'white hydrogen' as a fuel for the energy transition in the near future. Today, this potential role can only be apprehended on the basis of a few tangible but still incomplete geochemical data. The global atmospheric H_2 cycle has a global flux which is of the same order of magnitude as global H_2 demand. Within this cycle, the estimated solid Earth's contribution is small not to say negligible. Despite an increase of gaseous H_2 exploration activity which revealed diffuse H_2 at concentration above atmospheric background level in several places, no economically viable H_2 fields with several megatons of trapped gas has yet been revealed. Smaller H_2 gas accumulations may also prove economically viable if and only if the H_2 recharge rate is sufficient to allow commercially profitable exploitation, estimated here to several kton H_2 per year. The question becomes whether known natural H_2 formation processes have kinetics that would match the latter flow rate at the production well(s) and whether these processes are effective and stable over the time of the production operations. We approached this question by developing a model of H_2 production, transport and accumulation in an idealised aquifer, with the aim of recovering orders of magnitude. First, we show that only RedOx reactions involving the oxidation of iron contained in olivine in the presence of water (serpentinisation) can lead to the production of significant gaseous H_2. Radiolysis, although ubiquitous in continental environments, is far less efficient, except in uranium deposits. H_2 production from the high-temperature maturation of coals and shales after late hydrocarbon gas generation is complete (Horsfield et al., 2022) has not been considered here since it is not related to aquifer – rock interactions. Second, based on revisited thermodynamics data to model olivine low-temperature serpentinisation, we show that H_2 fluxes commensurable with gas production of economical interest are not achievable even in the most favorable case of deep production zones ($\geq$7,000 m). Gas accumulation is however possible, at relatively shallow levels (below a few hundred meters), provided that microbiological activity in the aquifer is about three-four orders of magnitude lower than expected from laboratory data and field measurements. We show that the combination of a deep H_2 source (7,000 m) and a shallow accumulation is the expected characteristic of a H_2 system in a cratonic setting associated with a deep aquifer. Owing to the major role played by microbial consumption in the gas accumulation rates, accumulation at 3,000 m would be highly favorable because of in-situ temperatures above the limit of microbial life considered here (100 °C). The relevant process that would allow H_2 gas saturation at 3,000 m would likely involve a production process at conditions beyond those considered here.

Geochemical data therefore tend to indicate that 'white H_2' is not renewable on the time scale of industrial exploitation (few decades) in the reference case of a deep aquifer setting. Yet, the role played by micro-organisms in the production and consumption of natural H_2 is probably the biggest unknown, on which the possibility of considering natural H_2 as a renewable energy source will certainly depend. The contribution of micro-organisms in soils as a major sink at the scale of the global atmospheric H_2 cycle suggests that this role should be important if not essential.

In conclusion, the present conceptual model of a deep aquifer fed by H_2 produced by ultramafic rocks (located in the bedrock) indicates that high-purity H_2 accumulations are expected at depths less than a few hundred meters in this type of geological and hydrological setting. As for hydrocarbon gas deposits, large H_2 accumulation with volumes sufficient to be economically exploitable are to be search for since significant recharge over the exploitation period seems unlikely.

Acknowledgements

Constructive comments by Frieder Klein, an anonymous reviewer and Jesse Walters (Handling Editor) were greatly appreciated and significantly helped improve the manuscript. D. I. Foustoukos is thanked for his help with the kinetic equation (1) and approval of the pre-exponential factor correction. L. Truche is thanked for enlightening discussions on the Bulqizë ophiolite. I. Moretti and A. Prinzhofer are thanked for sharing their knowledge of the H_2 dynamics in the São Francisco basin (Brazil).This work follows on from William Carlin's PhD work on H_2 source rocks in the São Francisco basin.

Data availability statement

No data or code were generated or analysed during this study. Figures and Tables numbers with an 'S', (e.g., Figure S1), additional details and input parameters for calculations are available in the Supplementary Materials which accompany the online version of this article.

Licence agreement

References

Abrajano T, Sturchio N, Bohlke J, Lyon G, Poreda R, Stevens C (1988). Methane-hydrogen gas seeps, Zambales Ophiolite, Philippines: Deep or shallow origin? *Chemical Geology* 71(1): 211–222. doi:10.1016/0009-2541(88)90116-7.

Ahmed AH, Arai S, Attia AK (2001). Petrological characteristics of podiform chromitites and associated peridotites of the Pan African Proterozoic ophiolite complexes of Egypt. *Mineralium Deposita* 36: 72–84. doi:10.1007/s001260050287.

Ahmed T (2018). *Reservoir Engineering Handbook*. Gulf Professional Publishing, 5th edn.

Aitken MJ (1985). Thermoluminescence dating: Past progress and future trends. *Nuclear Tracks and Radiation Measurements (1982)* 10(1): 3–6. doi:10.1016/0735-245X(85)90003-1.

Aquino KA, Perez Ad, Juego CMM, Tagle YGM, Leong JAM, Codillo EA (2025). High hydrogen outgassing from an ophiolite-hosted seep in Zambales, Philippines. *International Journal of Hydrogen Energy* 105: 360–366. doi:10.1016/j.ijhydene.2025.01.251.

Aresta M, Dibenedetto A (2024). Merging the Green-H_2 production with Carbon Recycling for stepping towards the Carbon Cyclic Economy. *Journal of CO_2 Utilization* 80: 102688. doi:10.1016/j.jcou.2024.102688.

Bagnoud A, Chourey K, Hettich RL, de Bruijn I, Andersson AF, Leupin OX, Schwyn B, Bernier-Latmani R (2016). Reconstructing a hydrogen-driven microbial metabolic network in Opalinus Clay rock. *Nature Communications* 7(1): 12770. doi:10.1038/ncomms12770.

Beard JS, Frost BR (2017). The stoichiometric effects of ferric iron substitutions in serpentine from microprobe data. *International Geology Review* 59(5-6): 541–547. doi:10.1080/00206814.2016.1197803.

Blay-Roger R, Bach W, Bobadilla LF, Reina TR, Odriozola JA, Amils R, Blay V (2024). Natural hydrogen in the energy transition: Fundamentals, promise, and enigmas. *Renewable and Sustainable Energy Reviews* 189: 113888. doi:10.1016/j.rser.2023.113888.

Bouquet A, Glein CR, Wyrick D, Waite JH (2017). Alternative Energy: Production of H_2 by Radiolysis of Water in the Rocky Cores of Icy Bodies. *The Astrophysical Journal Letters* 840(1): L8. doi:10.3847/2041-8213/aa6d56.

Brantley SL, Mellott NP (2000). Surface area and porosity of primary silicate minerals. *American Mineralogist* 85(11-12): 1767–1783. doi:10.2138/am-2000-11-1220.

Breznak JA, Switzer JM (1986). Acetate Synthesis from H_2 plus CO_2 by Termite Gut Microbes. *Applied and Environmental Microbiology* 52(4): 623–630. doi:10.1128/aem.52.4.623-630.1986.

Cannat M, Fontaine F, EscartíN J (2010). Serpentinization and Associated Hydrogen And Methane Fluxes at Slow Spreading Ridges. In *Diversity Of Hydrothermal Systems On Slow Spreading Ocean Ridges*, pp. 241–264. American Geophysical Union (AGU). doi:10.1029/2008GM000760.

Carlin W, Malvoisin B, Brunet F, Lanson B, Findling N, Lanson M, Fargetton T, Jeannin L, Lhote O (2024). Kinetics of low-temperature H_2 production in ultramafic rocks by ferroan brucite oxidation. *Geochemical Perspectives Letters* 29: 27–32. doi:10.7185/geochemlet.2408.

Charlou J, Donval J, Fouquet Y, Jean-Baptiste P, Holm N (2002). Geochemistry of high H_2 and CH_4 vent fluids issuing from ultramafic rocks at the Rainbow hydrothermal field (36° 14' N, MAR). *Chemical geology* 191(4): 345–359. doi:10.1016/S0009-2541(02)00134-1.

Charlou JL, Donval JP, Konn C, Ondréas H, Fouquet Y, Jean-Baptiste P, Fourré E (2010). High production and fluxes of H_2 and CH_4 and evidence of abiotic hydrocarbon synthesis by serpentinization in ultramafic-hosted hydrothermal systems on the Mid-Atlantic Ridge. *Geophysical Monograph Series* 188: 265–296. doi:10.1029/2008GM000752.

Conrad R (1996). Soil microorganisms as controllers of atmospheric trace gases (H_2, CO, CH_4, OCS, N_2O, and NO). *Microbiological reviews* 60(4): 609–640. doi:10.1128/mr.60.4.609-640.1996.

Conrad R, Seiler W (1981). Decomposition of atmospheric hydrogen by soil microorganisms and soil enzymes. *Soil Biology and Biochemistry* 13(1): 43–49. doi:10.1016/0038-0717(81)90101-2.

Constant P, Poissant L, Villemur R (2008). Isolation of Streptomyces sp. PCB7, the first microorganism demonstrating high-affinity uptake of tropospheric H_2. *The ISME Journal* 2(10): 1066–1076. doi:10.1038/ismej.2008.59.

Corre M, Brunet F, Schwartz S, Gautheron C, Agranier A, Lesimple S (2023). Quaternary low-temperature serpentinization and carbonation in the New Caledonia ophiolite. *Scientific Reports* 13(1): 19413. doi:10.1038/s41598-023-46691-y.

Derwent R, Simmonds P, O'Doherty S, Manning A, Collins W, Stevenson D (2006). Global environmental impacts of the hydrogen economy. *International Journal of Nuclear Hydrogen Production and Applications* 1(1): 57–67. doi:10.1504/IJNHPA.2006.009869.

Dick HJ (1974). Terrestrial nickel-iron from the Josephine peridotite, its geologic occurrence, associations, and origin. *Earth and Planetary Science Letters* 24(2): 291–298. doi:10.1016/0012-821X(74)90107-1.

Dohrmann AB, Krüger M (2023). Microbial H_2 Consumption by a Formation Fluid from a Natural Gas Field at High-Pressure Conditions Relevant for Underground H_2 Storage. *Environmental Science & Technology* 57(2): 1092–1102. doi:10.1021/acs.est.2c07303.

Dong Z, Layzell D (2001). H_2 oxidation, O_2 uptake and CO_2 fixation in hydrogen treated soils. *Plant and Soil* 229(1): 1–12. doi:10.1023/A:1004810017490.

Dubessy J, Pagel M, Beny JM, Christensen H, Hickel B, Kosztolanyi C, Poty B (1988). Radiolysis evidenced by H_2-O_2 and H_2-bearing fluid inclusions in three uranium deposits. *Geochimica et Cosmochimica Acta* 52(5): 1155–1167. doi:10.1016/0016-7037(88)90269-4.

Ehhalt DH, Rohrer F (2009). The tropospheric cycle of H_2: a critical review. *Tellus B: Chemical and Physical Meteorology* 61(3): 500–535. doi:10.1111/j.1600-0889.2009.00416.x.

Ellis GS, Gelman SE (2024). Model predictions of global geologic hydrogen resources. *Science Advances* 10(50): eado0955. doi:10.1126/sciadv.ado0955.

Fontecave M, Candel S, Poinsot T (2024). L'hydrogène aujourd'hui et demain. *Tech. rep.*, Académie des sciences (France). doi:10.62686/5.

Foustoukos DI, Houghton JL, Seyfried WE, Sievert SM, Cody GD (2011). Kinetics of H_2–O_2–H_2O redox equilibria and formation of metastable H_2O_2 under low temperature hydrothermal conditions. *Geochimica et Cosmochimica Acta* 75(6): 1594–1607. doi:10.1016/j.gca.2010.12.020.

Frery E, Langhi L, Maison M, Moretti I (2021). Natural hydrogen seeps identified in the North Perth Basin, Western Australia. *International Journal of Hydrogen Energy* 46(61): 31158–31173. doi:10.1016/j.ijhydene.2021.07.023.

Gaucher EC (2020). New Perspectives in the Industrial Exploration for Native Hydrogen. *Elements* 16(1): 8–9. doi:10.2138/gselements.16.1.8.

Geymond U, Briolet T, Combaudon V, Sissmann O, Martinez I, Duttine M, Moretti I (2023). Reassessing the role of magnetite during natural hydrogen generation. *Frontiers in Earth Science* 11. doi:10.3389/feart.2023.1169356.

Geymond U, Ramanaidou E, Lévy D, Ouaya A, Moretti I (2022). Can Weathering of Banded Iron Formations Generate Natural Hydrogen? Evidence from Australia, Brazil and South Africa. *Minerals* 12(2): 163. doi:10.3390/min12020163.

Greening C, Constant P, Hards K, Morales SE, Oakeshott JG, Russell RJ, Taylor MC, Berney M, Conrad R, Cook GM (2015). Atmospheric Hydrogen Scavenging: from Enzymes to Ecosystems. *Applied and Environmental Microbiology* 81(4): 1190–1199. doi:10.1128/AEM.03364-14.

Guélard J, Beaumont V, Rouchon V, Guyot F, Pillot D, Jézéquel D, Ader M, Newell KD, Deville E (2017). Natural H_2 in Kansas: Deep or shallow origin? *Geochemistry, Geophysics, Geosystems* 18(5): 1841–1865. doi:10.1002/2016GC006544.

Harris SH, Smith RL, Suflita JM (2007). In situ hydrogen consumption kinetics as an indicator of subsurface microbial activity: In situ microbial hydrogen consumption kinetics. *FEMS Microbiology Ecology* 60(2): 220–228. doi:10.1111/j.1574-6941.2007.00286.x.

Haumann FA, Batenburg AM, Pieterse G, Gerbig C, Krol MC, Röckmann T (2013). Emission ratio and isotopic signatures of molecular hydrogen emissions from tropical biomass burning. *Atmospheric Chemistry and Physics* 13(18): 9401–9413. doi:10.5194/acp-13-9401-2013.

Hofmann B (1992). Isolated reduction phenomena in red beds: A result of porewater radiolysis? In *International symposium on water-rock interaction, Park City, Utah, USA*, pp. 503–506.

Holloway JR, O'Day PA (2000). Production of CO_2 and H_2 by Diking-Eruptive Events at Mid-Ocean Ridges: Implications for Abiotic Organic Synthesis and Global Geochemical Cycling. *International Geology Review* 42(8): 673–683. doi:10.1080/00206810009465105.

Horsfield B, Mahlstedt N, Weniger P, Misch D, Vranjes-Wessely S, Han S, Wang C (2022). Molecular hydrogen from organic sources in the deep Songliao Basin, P.R. China. *International Journal of Hydrogen Energy* 47(38): 16750–16774. doi:10.1016/j.ijhydene.2022.02.208.

Hossain ME (2015). Drilling Costs Estimation for Hydrocarbon Wells. *Journal of Sustainable Energy Engineering* 3(1): 3–32. doi:10.7569/jsee.2014.629520.

Huang R, Lin CT, Sun W, Ding X, Zhan W, Zhu J (2017). The production of iron oxide during peridotite serpentinization: Influence of pyroxene. *Geoscience Frontiers* 8(6): 1311–1321. doi:10.1016/j.gsf.2017.01.001.

Huang R, Shang X, Zhao Y, Sun W, Liu X (2023). Effect of Fluid Salinity on Reaction Rate and Molecular Hydrogen (H_2) Formation During Peridotite Serpentinization at 300°C. *Journal of Geophysical Research: Solid Earth* 128(3): e2022JB025218. doi:10.1029/2022JB025218.

Huang R, Sun W, Song M, Ding X (2019). Influence of pH on Molecular Hydrogen (H_2) Generation and Reaction Rates during Serpentinization of Peridotite and Olivine. *Minerals* 9(11): 661. doi:10.3390/min9110661.

Häring V, Conrad R (1994). Demonstration of two different H_2-oxidizing activities in soil using an H_2 consumption and a tritium exchange assay. *Biology and Fertility of Soils* 17(2): 125–128. doi:10.1007/BF00337744.

Ivanova AE, Borzenkov IA, Tarasov AL, Milekhina EI, Belyaev SS (2007). A microbiological study of an underground gas storage in the process of gas injection. *Microbiology* 76(4): 453–460. doi:10.1134/S002626170704011X.

Jackson O, Lawrence SR, Hutchinson IP, Stocks AE, Barnicoat AC, Powney M (2024). Natural hydrogen: sources, systems and exploration plays. *Geoenergy* 2(1): geoenergy2024–002. doi:10.1144/geoenergy2024-002.

Janetz S, Jahnke C, Wendland F, Voigt HJ (2020). Modeling of groundwater flow velocity and aquifer recharge in a Cenozoic multi-aquifer system-a case study from Eastern Brandenburg (Germany). In *EGU General Assembly Conference Abstracts*, p. 21667. doi:10.5194/egusphere-egu2020-21667.

Johnson JW, Oelkers EH, Helgeson HC (1992). SUPCRT92: A software package for calculating the standard molal thermodynamic properties of minerals, gases, aqueous species, and reactions from 1 to 5000 bar and 0 to 1000°C. *Computers & Geosciences* 18(7): 899–947. doi:10.1016/0098-3004(92)90029-Q.

Kamdee K, Nantasin P, Chotpantarat S, Saengkorakot C, Chanruang P, Polee C, Khaweerat S, Uapoonphol N, Fungklin R, Sriwiang W, Kongsri S, Kukusamude C (2022). Assessment of groundwater dynamics in Quaternary aquifers of the Phrae Basin, northern Thailand, using isotope techniques. *Hydrogeology Journal* 30(4): 1091–1109. doi:10.1007/s10040-022-02478-5.

Keir RS (2010). A note on the fluxes of abiogenic methane and hydrogen from mid-ocean ridges. *Geophysical Research Letters* 37(24). doi:10.1029/2010GL045362.

Keller NS, Lüders K, Hornbruch G, Birnstengel S, Vogt C, Ebert M, Kallies R, Dahmke A, Richnow HH (2024). Rapid Consumption of Dihydrogen Injected into a Shallow Aquifer by Ecophysiologically Different Microbes. *Environmental Science & Technology* 58(1): 333–341. doi:10.1021/acs.est.3c04340.

Kita I, Matsuo S, Wakita H (1982). H_2 generation by reaction between H_2O and crushed rock: An experimental study on H_2 degassing from the active fault zone. *Journal of Geophysical Research: Solid Earth* 87(B13): 10789–10795. doi:10.1029/JB087iB13p10789.

Klein F, Bach W, Humphris SE, Kahl WA, Jöns N, Moskowitz B, Berquó TS (2014). Magnetite in seafloor serpentinite—Some like it hot. *Geology* 42(2): 135–138. doi:10.1130/G35068.1.

Klein F, Grozeva NG, Seewald JS (2019). Abiotic methane synthesis and serpentinization in olivine-hosted fluid inclusions. *Proceedings of the National Academy of Sciences* 116(36): 17666–17672. doi:10.1073/pnas.1907871116.

Klein F, Tarnas J, Bach W (2020). Abiotic Sources of Molecular Hydrogen on Earth. *Elements* 16: 24. doi:10.2138/gselements.16.1.19.

Le Caër S (2011). Water Radiolysis: Influence of Oxide Surfaces on H_2 Production under Ionizing Radiation. *Water* 3(1): 235–253. doi:10.3390/w3010235.

Lee B, Lee H, Lim D, Brigljević B, Cho W, Cho HS, Kim CH, Lim H (2020). Renewable methanol synthesis from renewable H_2 and captured CO_2: How can power-to-liquid technology be economically feasible? *Applied Energy* 279: 115827. doi:10.1016/j.apenergy.2020.115827.

Lefeuvre N, Truche L, Donzé FV, Ducoux M, Barré G, Fakoury RA, Calassou S, Gaucher EC (2021). Native H_2 Exploration in the Western Pyrenean Foothills. *Geochemistry, Geophysics, Geosystems* 22(8): e2021GC009917. doi:10.1029/2021GC009917.

Leila M, Loiseau K, Moretti I (2022). Controls on generation and accumulation of blended gases (CH_4/H_2/He) in the Neoproterozoic Amadeus Basin, Australia. *Marine and Petroleum Geology* 140: 105643. doi:10.1016/j.marpetgeo.2022.105643.

Leong JA, Nielsen M, McQueen N, Karolytė R, Hillegonds DJ, Ballentine C, Darrah T, McGillis W, Kelemen P (2023). H_2 and CH_4 outgassing rates in the Samail ophiolite, Oman: Implications for low-temperature, continental serpentinization rates. *Geochimica et Cosmochimica Acta* 347: 1–15. doi:10.1016/j.gca.2023.02.008.

Levitt CJ (2016). Information spillovers in onshore oil and gas exploration. *Resource and Energy Economics* 45: 80–98. doi:10.1016/j.reseneeco.2016.05.003.

Lévy D, Roche V, Pasquet G, Combaudon V, Geymond U, Loiseau K, Moretti I (2023). Natural H_2 exploration: tools and workflows to characterize a play. *Science and Technology for Energy Transition* 78: 27. doi:10.2516/stet/2023021.

Li S, Djilali N, Rosen MA, Crawford C, Sui PC (2022). Transition of heavy-duty trucks from diesel to hydrogen fuel cells: Opportunities, challenges, and recommendations. *International Journal of Energy Research* 46(9): 11718–11729. doi:10.1002/er.8066.

Lin LH, Hall J, Lippmann-Pipke J, Ward JA, Lollar BS, DeFlaun M, Rothmel R, Moser D, Gihring TM, Mislowack B, Onstott TC (2005a). Radiolytic H_2 in continental crust: Nuclear power for deep subsurface microbial communities. *Geochemistry, Geophysics, Geosystems* 6(7). doi:10.1029/2004GC000907.

Lin LH, Slater GF, Lollar BS, Lacrampe-Couloume G, Onstott TC (2005b). The yield and isotopic composition of radiolytic H_2, a potential energy source for the deep subsurface biosphere. *Geochimica et Cosmochimica Acta* 69(4): 893–903. doi:10.1016/j.gca.2004.07.032.

Lollar BS, Onstott TC, Lacrampe-Couloume G, Ballentine CJ (2014). The contribution of the Precambrian continental lithosphere to global H_2 production. *Nature* 516(7531): 379–382. doi:10.1038/nature14017.

Lopez-Lazaro C, Bachaud P, Moretti I, Ferrando N (2019). Predicting the phase behavior of hydrogen in NaCl brines by molecular simulation for geological applications. *Bulletin de la Société Géologique de France* 190(1): 7. doi:10.1051/bsgf/2019008.

Löffler M, Schrader M, Lüders K, Werban U, Hornbruch G, Dahmke A, Vogt C, Richnow HH (2022). Stable Hydrogen Isotope Fractionation of Hydrogen in a Field Injection Experiment: Simulation of a Gaseous H_2 Leakage. *ACS Earth and Space Chemistry* 6(3): 631–641. doi:10.1021/acsearthspacechem.1c00254.

Maiga O, Deville E, Laval J, Prinzhofer A, Diallo AB (2023). Characterization of the spontaneously recharging natural hydrogen reservoirs of Bourakebougou in Mali. *Scientific Reports* 13(1): 11876. doi:10.1038/s41598-023-38977-y.

Malvoisin B, Brunet F (2023). Barren ground depressions, natural H_2 and orogenic gold deposits: Spatial link and geochemical model. *Science of The Total Environment* 856: 158969. doi:10.1016/j.scitotenv.2022.158969.

Marcaillou C, Muñoz M, Vidal O, Parra T, Harfouche M (2011). Mineralogical evidence for H_2 degassing during serpentinization at 300°C/300bar. *Earth and Planetary Science Letters* 303(3-4): 281–290. doi:10.1016/j.epsl.2011.01.006.

Mayhew LE, Ellison ET (2020). A synthesis and meta-analysis of the Fe chemistry of serpentinites and serpentine minerals. *Philosophical Transactions of the Royal Society A: Mathematical, Physical and Engineering Sciences* 378(2165): 20180420–20180420. doi:10.1098/rsta.2018.0420.

McCollom TM (2003). Formation of meteorite hydrocarbons from thermal decomposition of siderite ($FeCO_3$). *Geochimica et Cosmochimica Acta* 67(2): 311–317. doi:10.1016/S0016-7037(02)00945-6.

McCollom TM, Bach W (2009). Thermodynamic constraints on hydrogen generation during serpentinization of ultramafic rocks. *Geochimica et Cosmochimica Acta* 73(3): 856–875. doi:10.1016/j.gca.2008.10.032.

McCollom TM, Donaldson C (2016). Generation of Hydrogen and Methane during Experimental Low-Temperature Reaction of Ultramafic Rocks with Water. *Astrobiology* 16(6): 389–406. doi:10.1089/ast.2015.1382.

Milesi V, Guyot F, Brunet F, Richard L, Recham N, Benedetti M, Dairou J, Prinzhofer A (2015). Formation of CO_2, H_2 and condensed carbon from siderite dissolution in the 200–300 °C range and at 50 MPa. *Geochimica et Cosmochimica Acta* 154: 201–211. doi:10.1016/j.gca.2015.01.015.

Milesi V, Prinzhofer A, Guyot F, Benedetti M, Rodrigues R (2016). Contribution of siderite–water interaction for the unconventional generation of hydrocarbon gases in the Solimões basin, northwest Brazil. *Marine and Petroleum Geology* 71: 168–182. doi:10.1016/j.marpetgeo.2015.12.022.

Miller HM, Mayhew LE, Ellison ET, Kelemen P, Kubo M, Templeton AS (2017). Low temperature hydrogen production during experimental hydration of partially-serpentinized dunite. *Geochimica et Cosmochimica Acta* 209: 161–183. doi:10.1016/j.gca.2017.04.022.

Moody JB (1976). Serpentinization: a review. *Lithos* 9(2): 125–138. doi:10.1016/0024-4937(76)90030-X.

Moretti I (2019). H_2: energy vector or source? *L'Actualité Chimique* 442: 15–16. URL https://new.societechimiquedefrance.fr/numero/h2-vecteur-ou-source-denergie-p15-n442/.

Moretti I, Brouilly E, Loiseau K, Prinzhofer A, Deville E (2021a). Hydrogen Emanations in Intracratonic Areas: New Guide Lines for Early Exploration Basin Screening. *Geosciences* 11(3): 145. doi:10.3390/geosciences11030145.

Moretti I, Geymond U, Pasquet G, Aimar L, Rabaute A (2022). Natural hydrogen emanations in Namibia: Field acquisition and vegetation indexes from multispectral satellite image analysis. *International Journal of Hydrogen Energy* 47(84): 35588–35607. doi:10.1016/j.ijhydene.2022.08.135.

Moretti I, Prinzhofer A, Françolin J, Pacheco C, Rosanne M, Rupin F, Mertens J (2021b). Long-term monitoring of natural hydrogen superficial emissions in a brazilian cratonic environment. Sporadic large pulses versus daily periodic emissions. *International Journal of Hydrogen Energy* 46(5): 3615–3628. doi:10.1016/j.ijhydene.2020.11.026.

Mouli-Castillo J, Heinemann N, Edlmann K (2021). Mapping geological hydrogen storage capacity and regional heating demands: An applied UK case study. *Applied Energy* 283: 116348. doi:10.1016/j.apenergy.2020.116348.

Moussallam Y, Oppenheimer C, Aiuppa A, Giudice G, Moussallam M, Kyle P (2012). Hydrogen emissions from Erebus volcano, Antarctica. *Bulletin of Volcanology* 74: 2109–2120. doi:10.1007/s00445-012-0649-2.

Myagkiy A, Brunet F, Popov C, Krüger R, Guimarães H, Sousa RS, Charlet L, Moretti I (2020). H_2 dynamics in the soil of a H_2-emitting zone (São Francisco Basin, Brazil): Microbial uptake quantification and reactive transport modelling. *Applied Geochemistry* 112: 104474. doi:10.1016/j.apgeochem.2019.104474.

Neal C, Stanger G (1983). Hydrogen generation from mantle source rocks in Oman. *Earth and Planetary Science Letters* 66: 315–320. doi:10.1016/0012-821X(83)90144-9.

Novelli PC, Lang PM, Masarie KA, Hurst DF, Myers R, Elkins JW (1999). Molecular hydrogen in the troposphere: Global distribution and budget. *Journal of Geophysical Research: Atmospheres* 104(D23): 30427–30444. doi:10.1029/1999JD900788.

Ocko IB, Hamburg SP (2022). Climate consequences of hydrogen emissions. *Atmospheric Chemistry and Physics* 22(14): 9349–9368. doi:10.5194/acp-22-9349-2022.

Oliveira AM, Beswick RR, Yan Y (2021). A green hydrogen economy for a renewable energy society. *Current Opinion in Chemical Engineering* 33: 100701. doi:10.1016/j.coche.2021.100701.

Patonia A, Lambert M, Lin N, Shuster M, Austin B (2024). Natural (geologic) hydrogen and its potential role in a net-zero carbon future: Is all that glitters gold? *Oxford Institute of Energy Studies Paper* ET38.

Patterson JD, Aydin M, Crotwell AM, Petron G, Severinghaus JP, Saltzman ES (2020). Atmospheric History of H_2 Over the Past Century Reconstructed From South Pole Firn Air. *Geophysical Research Letters* 47(14): e2020GL087787. doi:10.1029/2020GL087787.

Pedersen K (1997). Microbial life in deep granitic rock. *FEMS Microbiology Reviews* 20(3-4): 399–414. doi:10.1111/j.1574-6976.1997.tb00325.x.

Penner JE, McElroy MB, Wofsy SC (1977). Sources and sinks for atmospheric H_2: A current analysis with projections for the influence of anthropogenic activity. *Planetary and Space Science* 25(6): 521–540. doi:10.1016/0032-0633(77)90059-9.

Price H, Jaeglé L, Rice A, Quay P, Novelli PC, Gammon R (2007). Global budget of molecular hydrogen and its deuterium content: Constraints from ground station, cruise, and aircraft observations. *Journal of Geophysical Research: Atmospheres* 112(D22). doi:10.1029/2006JD008152.

Prinzhofer A, Cacas-Stentz MC (2023). Natural hydrogen and blend gas: a dynamic model of accumulation. *International Journal of Hydrogen Energy* 48(57): 21610–21623. doi:10.1016/j.ijhydene.2023.03.060.

Prinzhofer A, Moretti I, Françolin J, Pacheco C, D'Agostino A, Werly J, Rupin F (2019). Natural hydrogen continuous emission from sedimentary basins: The example of a Brazilian H_2-emitting structure. *International Journal of Hydrogen Energy* 44(12): 5676–5685. doi:10.1016/j.ijhydene.2019.01.119.

Prinzhofer A, Tahara Cissé CS, Diallo AB (2018). Discovery of a large accumulation of natural hydrogen in Bourakebougou (Mali). *International Journal of Hydrogen Energy* 43(42): 19315–19326. doi:10.1016/j.ijhydene.2018.08.193.

Robinson JA, Tiedje JM (1984). Competition between sulfate-reducing and methanogenic bacteria for H_2 under resting and growing conditions. *Archives of Microbiology* 137(1): 26–32. doi:10.1007/BF00425803.

van Ruijven B, Lamarque JF, van Vuuren DP, Kram T, Eerens H (2011). Emission scenarios for a global hydrogen economy and the consequences for global air pollution. *Global Environmental Change* 21(3): 983–994. doi:10.1016/j.gloenvcha.2011.03.013.

Saidy K, Fawad M, Whattam SA, Al-Shuhail AA, Al-Shuhail AA, Campos M, Sulistyohariyanto FA (2024). Unlocking the H_2 potential in Saudi Arabia: Exploring serpentinites as a source of H_2 production. *International Journal of Hydrogen Energy* 89: 1482–1491. doi:10.1016/j.ijhydene.2024.09.256.

Sato M, Sutton AJ, McGee KA (1984). Anomalous hydrogen emissions from the San Andreas fault observed at the Cienega Winery, central California. *pure and applied geophysics* 122(2): 376–391. doi:10.1007/BF00874606.

Savary V, Pagel M (1997). The effects of water radiolysis on local redox conditions in the Oklo, Gabon, natural fission reactors 10 and 16. *Geochimica et Cosmochimica Acta* 61(21): 4479–4494. doi:10.1016/S0016-7037(97)00261-5.

Schmidt U (1974). Molecular hydrogen in the atmosphere. *Tellus* 26(1-2): 78–90. doi:10.1111/j.2153-3490.1974.tb01954.x.

Schultz MG, Diehl T, Brasseur GP, Zittel W (2003). Air Pollution and Climate-Forcing Impacts of a Global Hydrogen Economy. *Science* 302(5645): 624–627. doi:10.1126/science.1089527.

Schwarzenbach EM, Vrijmoed JC, Engelmann JM, Liesegang M, Wiechert U, Rohne R, Plümper O (2021). Sulfide Dissolution and Awaruite Formation in Continental Serpentinization Environments and Its Implications to Supporting Life. *Journal of Geophysical Research: Solid Earth* 126(5): e2021JB021758. doi:10.1029/2021JB021758.

Schönauer AL, Glanz S (2022). Hydrogen in future energy systems: Social acceptance of the technology and its large-scale infrastructure. *International Journal of Hydrogen Energy* 47(24): 12251–12263. doi:10.1016/j.ijhydene.2021.05.160.

Seward T, Franck E (1981). The system hydrogen-water up to 440 C and 2500 bar pressure. *Berichte der Bunsengesellschaft für physikalische Chemie* 85(1): 2–7. doi:10.1002/bbpc.19810850103.

Seyfried WE, Foustoukos DI, Fu Q (2007). Redox evolution and mass transfer during serpentinization: An experimental and theoretical study at 200 °C, 500 bar with implications for ultramafic-hosted hydrothermal systems at Mid-Ocean Ridges. *Geochimica et Cosmochimica Acta* 71(15): 3872–3886. doi:10.1016/j.gca.2007.05.015.

Shahien MG, Azer MK, Asimow PD (2021). Neoproterozoic Ophiolites of the Arabian-Nubian Shield. In Hamimi Z, Fowler AR, Liégeois JP, Collins A, Abdelsalam MG, Abd El-Wahed M (eds.) *The Geology of the Arabian-Nubian Shield*, pp. 297–330. Springer International Publishing, Cham. doi:10.1007/978-3-030-72995-0_12.

Thaysen EM, McMahon S, Strobel GJ, Butler IB, Ngwenya BT, Heinemann N, Wilkinson M, Hassanpouryouzband A, McDermott CI, Edlmann K (2021). Estimating microbial growth and hydrogen consumption in hydrogen storage in porous media. *Renewable and Sustainable Energy Reviews* 151: 111481. doi:10.1016/j.rser.2021.111481.

Truche L, Donzé FV, Goskolli E, Muceku B, Loisy C, Monnin C, Dutoit H, Cerepi A (2024). A deep reservoir for hydrogen drives intense degassing in the Bulqizë ophiolite. *Science* 383(6683): 618–621. doi:10.1126/science.adk9099.

Vacquand C, Deville E, Beaumont V, Guyot F, Sissmann O, Pillot D, Arcilla C, Prinzhofer A (2018). Reduced gas seepages in ophiolitic complexes: Evidences for multiple origins of the H_2-CH_4-N_2 gas mixtures. *Geochimica et Cosmochimica Acta* 223: 437–461. doi:10.1016/j.gca.2017.12.018.

Vollmer MK, Walter S, Mohn J, Steinbacher M, Bond SW, Röckmann T, Reimann S (2012). Molecular hydrogen (H_2) combustion emissions and their isotope (D/H) signatures from domestic heaters, diesel vehicle engines, waste incinerator plants, and biomass burning. *Atmospheric Chemistry and Physics* 12(14): 6275–6289. doi:10.5194/acp-12-6275-2012.

Wakita H, Nakamura Y, Kita I, Fujii N, Notsu K (1980). Hydrogen Release: New Indicator of Fault Activity. *Science* 210(4466): 188–190. doi:10.1126/science.210.4466.188.

Warneck P (1988). Chapter 6 Volatile Hydrocarbons and Halocarbons. In Dmowska R, Holton JR, Rossby HT (eds.) *Chemistry of the Natural Atmosphere*, vol. 41 of *International Geophysics*, pp. 223–277. Academic Press. doi:10.1016/S0074-6142(08)60633-6.

Wei HF, Ledoux E, De Marsily G (1990). Regional modelling of groundwater flow and salt and environmental tracer transport in deep aquifers in the Paris Basin. *Journal of Hydrology* 120(1): 341–358. doi:10.1016/0022-1694(90)90158-T.

Worman SL, Pratson LF, Karson JA, Klein EM (2016). Global rate and distribution of H_2 gas produced by serpentinization within oceanic lithosphere. *Geophysical Research Letters* 43(12): 6435–6443. doi:10.1002/2016GL069066.

Wu S, Salmon N, Li MMJ, Bañares-Alcántara R, Tsang SCE (2022). Energy Decarbonization via Green H_2 or NH_3? *ACS Energy Letters* 7(3): 1021–1033. doi:10.1021/acsenergylett.1c02816.

Zgonnik V (2020). The occurrence and geoscience of natural hydrogen: A comprehensive review. *Earth-Science Reviews* 203: 103140. doi:10.1016/j.earscirev.2020.103140.

Zgonnik V, Beaumont V, Larin N, Pillot D, Deville E (2019). Diffused flow of molecular hydrogen through the Western Hajar mountains, Northern Oman. *Arabian Journal of Geosciences* 12(3): 71. doi:10.1007/s12517-019-4242-2.

Zhu J, Tao R, Ishii T, Ikuta D, Xu W, Zhang L, Su Y, Liu R, Jin Z (2025). Iron hydride (FeHx) as a crucial intermediate in transformation of subducted H_2O to abiotic H_2 in Earth's deep mantle. *Science China Earth Sciences* 68: 1485–1496. doi:10.1007/s11430-024-1544-6.

Zimmer M, Kröner A, Jochum K, Reischmann T, Todt W (1995). The Gabal Gerf complex: a Precambrian N-MORB ophiolite in the Nubian shield, NE Africa. *Chemical Geology* 123(1-4): 29–51. doi:10.1016/0009-2541(95)00018-H.